NATIONAL ADVISORY COMMITTEE FOR AERONAUTICS

TECHNICAL NOTE 2248

ANALYSIS OF THE EFFECTS OF DESIGN PRESSURE RATIO PER STAGE AND OFF-DESIGN EFFICIENCY ON THE OPERATING RANGE OF MULTISTAGE AXIAL-FLOW COMPRESSORS

By Melvyn Savage and Willard R. Westphal

Langley Aeronautical Laboratory
Langley Field, Va.

Washington
December 1950

NATIONAL ADVISORY COMMITTEE FOR AERONAUTICS

TECHNICAL NOTE 2248

ANALYSIS OF THE EFFECTS OF DESIGN PRESSURE RATIO PER STAGE AND OFF-DESIGN EFFICIENCY ON THE OPERATING RANGE OF MULTISTAGE AXIAL-FLOW COMPRESSORS

By Melvyn Savage and Willard R. Westphal

SUMMARY

An equation is derived which expresses the polytropic efficiency necessary to maintain the design axial-velocity ratio across one or several blade rows of a compressor as a function of the design efficiency, the design static-pressure ratio, and the off-design static-pressure ratio. This equation is applied to the two-dimensional general case of a compressor rotor and is derived as a function of the stage design parameters. For a symmetrical stage, calculations are completed to determine these hypothetical necessary efficiencies at several off-design inlet axial velocities for a range of design pressure ratios. At high design pressure ratios, the reduction in hypothetical efficiency with decreasing inlet axial velocity was small enough to permit a possible matching of blade-row and hypothetical efficiencies.

The effects of design pressure ratio on axial-velocity change across a rotor at mass flows below design were further investigated by assuming the off-design blade-row efficiency to be constant. Calculations indicated that a greater reduction in axial velocity occurred across rotors having lower design pressure ratios. Hence, if it is assumed that the blade-row efficiency curves for high- and low-pressure-ratio designs are somewhat similar, a multistage compressor composed of high-pressure-ratio stages, operating with constant rotational speed at mass flows below design, will have higher off-design efficiencies and a wider mass-flow operating range than one made up of low-pressure-ratio stages.

INTRODUCTION

In the field of multistage axial-flow compressors, more information is needed on compressor performance at off-design mass flows. The ability to predict off-design performance of a multistage compressor by examination of the single-stage or single-blade-row characteristics is

very desirable. From an analytical point of view, being able to work with a single stage or a blade row reduces the complexity of the problem considerably. In any testing program, a single blade row or stage is easier to test than a multistage compressor.

Little work has been done on the analytical phase of predicting off-design performance of axial-flow multistage compressors from single-stage or single-blade-row characteristics. Once the effects of the single-stage characteristics are better understood, multistage compressors having specific off-design characteristics can probably be designed. For some applications, multistage axial-flow compressors having high over-all efficiency over a wide operating range may be desired. In other applications, it may be more desirable for a multistage compressor to have steep characteristic curves.

In reference 1, calculations were carried out to obtain the performance of 6-, 8-, and 13-stage axial-flow compressors, each designed for the same mass flow, rotational speed, and over-all pressure ratio. These calculations showed that, for a high-pressure-ratio stage having a rapid decrease in efficiency with decreasing mass flow, the increase in temperatures due to the inefficiency is sufficient to decrease the density ratio despite the increased pressure ratio. The axial velocity through the compressor thereby increases contrary to the usual phenomena observed in designs having lower pressure ratios per stage.

If compressors composed of high- or low-pressure-ratio stages are to be compared with the intention of determining which compressor has the widest mass-flow operating range and highest off-design efficiencies at various rotational speeds, the effects of design stage pressure ratio on all factors governing the off-design performance of the multistage compressor must be known. The effects of pressure ratio on the compressor peak-efficiency point, boundary-layer growth, surge line, secondary flow losses, and blade-row efficiency must be evaluated. Evaluating all these effects would present a very complex problem; therefore, it was decided to isolate and investigate one phase of the over-all problem. The purpose of this investigation was to determine how the operating range and over-all efficiency of a multistage axial-flow compressor are affected by the off-design efficiency characteristics of the blade row and the design pressure ratio. The analysis is simplified by assuming that the flow through the blade rows is two-dimensional. The flow is assumed to be compressible. The efficiency considered throughout the analysis is the blade-row efficiency expressed as a polytropic efficiency.

The technique used in the analysis was to define a hypothetical efficiency, which was the efficiency that would be necessary to maintain the design axial-velocity ratio across a blade row at various off-design mass flows as a function of blade-row design parameters. Since the

differences between this hypothetical efficiency and the actual blade-row efficiency curves determine the variation in axial velocity through the compressor at various off-design mass flows, the effects of design pressure ratio on the hypothetical efficiency curve were investigated. General analytic expressions for the hypothetical efficiency as a function of the rotor design parameters were derived. By examining these expressions, the effects of design pressure ratio and efficiency on both the operating range and the over-all efficiency were determined.

No attempt was made to analyze the stage efficiency to determine what part of the stage inefficiency may be attributed to vorticity produced by the previous stages or to boundary-layer growth.

SYMBOLS

A	annulus area
$\left(\frac{A_1}{A_2}\right)_f$	flow-area ratio across a two-dimensional cascade
a	velocity of sound
c_p	specific heat of gas at constant pressure
c_v	specific heat of gas at constant volume
M	Mach number
n	polytropic exponent for compression
p	static pressure
R	gas constant
t	static temperature
T	total temperature
U	rotational speed of rotor
V	velocity of air in stator coordinates
W	velocity of air in rotor coordinates

x ratio of off-design static-pressure ratio to design static-pressure ratio $\left(\frac{p_e/p_i}{(p_e/p_i)_D}\right)$

β angle between compressor axis and air-inlet velocity in rotor coordinates

γ ratio of specific heats (c_p/c_v)

δ angle between compressor axis and air-inlet velocity in stator coordinates

η small-stage or polytropic efficiency

η_n efficiency necessary to maintain design density ratio $(\rho_2/\rho_1)_D$ and design axial-velocity ratio $(V_{a_2}/V_{a_1})_D$ across a rotor at various off-design mass flows

θ turning angle in rotor coordinates

ρ static density

Subscripts:

1 in front of rotor

2 behind rotor

a axial

D design condition; symbols without subscript D are for off-design conditions

e any exit station

i any inlet station

r rotor reference frame

s stator reference frame

ANALYSIS AND DISCUSSION

Efficiency Necessary to Maintain Design Density Ratio at Off-Design Mass Flows

The exit axial velocity of a single stage in an axial-flow compressor is, of course, affected by the polytropic blade-row efficiency. If a stage is designed to produce a given pressure ratio with a certain efficiency and axial-velocity ratio $\left(V_{a_i}/V_{a_e}\right)_D$, that is, density ratio $\left(\rho_e/\rho_i\right)_D$, efficiencies can be found which will maintain this same design axial-velocity or density ratio at various off-design mass flows. The increase in static temperature due to the inefficiency causes a decrease in density which counteracts the density increase associated with an increase in pressure.

The flow through a compressor may be represented by an irreversible adiabatic process from station i to e which satisfies $\frac{p}{\rho^n}$ = Constant. This process will herein be called a polytropic process and the pressure-density relationship is given by the familiar polytropic relation:

$$\frac{p_e}{p_i} = \left(\frac{\rho_e}{\rho_i}\right)^n \tag{1}$$

The polytropic exponent n may be expressed in terms of the polytropic efficiency (reference 2):

$$\eta = \frac{\frac{\gamma - 1}{\gamma}}{\frac{n - 1}{n}} \tag{2}$$

When equations (1) and (2) are combined and the desired condition that the off-design density ratio be equal to the design density ratio is used, the following equation (see appendix A for derivation) results:

$$\frac{p_e/p_i}{\left(p_e/p_i\right)_D} = \left(\frac{p_e}{p_i}\right)_D^{\left[\frac{\frac{\gamma-1}{\gamma}\left(\frac{1}{\eta}-\frac{1}{\eta_D}\right)}{1-\frac{1}{\eta}\frac{\gamma-1}{\gamma}}\right]} \tag{3}$$

Equation (3) states that, for a given design efficiency and off-design static-pressure ratio, the efficiency required to maintain the design axial-velocity ratio at off-design conditions is a function only of the design static-pressure ratio. This necessary or required efficiency is denoted as η_n. Hence, by letting

$$x = \frac{p_e/p_i}{\left(p_e/p_i\right)_D}$$

equation (3) can be written as follows:

$$x = \left(\frac{p_e}{p_i}\right)_D^{\left[\frac{\frac{\gamma-1}{\gamma}\left(\frac{1}{\eta_n}-\frac{1}{\eta_D}\right)}{1-\frac{1}{\eta_n}\frac{\gamma-1}{\gamma}}\right]} \tag{4}$$

This expression is general in that stations i and e may be across a rotor, a stator, a stage, or several stages.

Figure 1 is a plot of equation (4) for $\eta_D = 0.90$ and for a range of $\left(p_2/p_1\right)_D$ values from 1.1 to 1.6. From this figure, the reduction in η_n with increasing x is less rapid for high-pressure-ratio stages than for low-pressure-ratio stages.

If the stage efficiency curve coincided with the curve for η_n of figure 1, the off-design axial-velocity ratios of the stages and of the whole compressor would be the same as at design. For example, if a multistage compressor designed to maintain constant axial velocity from stage to stage were operating with an inlet axial velocity 10 percent below design, the exit axial velocity would also be 10 percent below design.

If the η_n curve is lower than the actual stage efficiency curve (see point A, fig. 2(a)), at mass flows below design and with constant rotational speed assumed,

$$\frac{V_{a_e}}{V_{a_i}} < \left(\frac{V_{a_e}}{V_{a_i}}\right)_D$$

For constant axial velocity at design the following stage operates at a lower axial-velocity ratio $\frac{V_{a_i}}{(V_{a_i})_D}$ and efficiency. Each succeeding stage operates at a lower axial-velocity ratio as indicated in figure 2(a) until the stall point is reached. This situation is usual in multistage compressors made up of low-pressure-ratio stages and results in a very narrow mass-flow range for a given rotational speed.

If the η_n curve is higher than the actual stage efficiency curve (see point A, fig. 2(b)), at mass flows below design and with constant rotational speed assumed,

$$\frac{V_{a_e}}{V_{a_i}} > \left(\frac{V_{a_e}}{V_{a_i}}\right)_D$$

For constant axial velocity at design the following stage operates at a higher axial-velocity ratio $\frac{V_{a_i}}{(V_{a_i})_D}$ and efficiency. Each succeeding stage operates at a higher axial-velocity ratio and efficiency as indicated from A to B in figure 2(b). The lowest axial velocity at off-design flows is in the first stage. Therefore, this condition of η_n being higher than off-design stage efficiency tends to give high-efficiency off-design operation, a wide mass-flow operating range, and, in general, a flat characteristic curve.

If the η_n curve is lower than the actual blade-row efficiency curve for both high- and low-pressure-ratio stages and the blade-row efficiency curves for the two pressure ratios are assumed to be approximately the same, the difference between the stage efficiency and η_n would be less for high-pressure-ratio stages than for low-pressure-ratio stages since the curve for η_n is closer to horizontal for high pressure ratios (fig. 1). If the design axial velocity is constant, then at below-design mass flows the drop in axial velocity through a multistage compressor made up of low-pressure-ratio stages would be greater than in one made up of high-pressure-ratio stages. From available low-speed test data, the assumption of the similarity of blade-row efficiencies for high- and low-pressure-ratio stages appears to be justifiable (reference 3). Unpublished data on rotors having high pressure ratios indicate that the blade-row efficiency curve for high pressure ratios is flatter than for lower pressure ratios, but the difference between these efficiency curves is generally not as large as that existing between the η_n curves associated with the two design pressure ratios.

It might be necessary to steepen the characteristic curve of a multistage compressor in matching the compressor and turbine performance in a gas turbine engine. The characteristic curve can be steepened by increasing the difference between the blade-row efficiency and the η_n curves.

The preceding paragraphs were concerned with mass flows below design. Figure 2 indicates that, for mass flows greater than design, the difference between the assumed stage efficiency and η_n gets large very rapidly. For either high or low pressure ratios per stage, when the mass flow is greater than design, the succeeding stages operate farther down the stage efficiency curve. In these stages, the axial velocities would increase so that both lower stage pressure ratios and stage efficiencies would result. Consequently, the off-design over-all efficiency would be low.

It is impossible, therefore, to maintain the design axial-velocity ratio for mass flows greater than design unless the design point is chosen on the low-flow side of the stage peak-efficiency point.

General Expression for η_n across a Rotor as a Function of Blade-Row Parameters

In the application of equation (4) to an actual stage design, x must be found as a function of $\frac{V_{a_e}/V_{a_i}}{\left(V_{a_e}/V_{a_i}\right)_D}$. In obtaining a functional relationship between pressure ratios and axial velocities, blade-row parameters such as U, β, θ, and δ must be introduced. In effect, therefore, η_n must be known as a function of $\left(p_2/p_1\right)_D$, V_{a_1}, U, δ, and θ.

Figure 1 presents η_n against x for various design pressure ratios. The solid curve in figure 3 is such a curve for a specific design pressure ratio. The static-pressure ratio across a rotor is a function of V_{a_1}, T_{1_s}, U, δ, θ, and η. At the various off-design mass flows, this ratio may be simplified into $\frac{p_2}{p_1} = f\left(V_{a_1},\theta,\eta\right)$ inasmuch as T_{1_s}, U, and δ are constant for a particular design. For V_{a_1} equal to 0.95, 0.90, 0.85, and 0.80 of $\left(V_{a_1}\right)_D$, since the design velocity diagram is known, the corresponding values of β may be determined. For the known value of $d\theta/d\beta$, the values of θ are determined.

Then, $\frac{p_2}{p_1} = f(\eta)$ or $x = f(\eta)$; the dashed curves in figure 3 represent this functional relationship. The intersections indicated by a, b, c, and d define the η_n corresponding to each of the off-design inlet axial velocities. Curves of η_n against $V_{a_1}/(V_{a_1})_D$ for various design pressure ratios are presented subsequently.

The derivation of an expression for $\frac{p_2}{p_1} = f(M_{1_r}, \eta, \beta, \theta)$ may be found in appendix B. In this appendix, the ratios T_{1_r}/t_1 and T_{2_r}/t_2 were written as functions of M_{1_r} and M_{2_r}. Since $T_{1_r} = T_{2_r}$ and with the use of the polytropic equation relating t_2/t_1 to p_2/p_1,

$$\left(\frac{p_2}{p_1}\right)^{\frac{\gamma-1}{\eta\gamma}} = \frac{1 + \frac{\gamma - 1}{2} M_{1_r}^2}{1 + \frac{\gamma - 1}{2} M_{2_r}^2} \tag{5}$$

By means of the continuity equation

$$\left(\frac{A_1}{A_2}\right)_f = \frac{\rho_2}{\rho_1} \frac{V_{a_2} \cos \beta}{V_{a_1} \cos(\beta - \theta)} = \frac{\rho_2}{\rho_1} \frac{M_{2_r}}{M_{1_r}} \frac{\sqrt{t_2}}{\sqrt{t_1}} \tag{6}$$

M_{2_r} may be expressed as a function of p_2/p_1, $(A_2/A_1)_f$, and η. Combining this expression for M_{2_r} with equation (5) gives

$$\left(\frac{A_1}{A_2}\right)_f = \frac{1}{M_{1_r}} \sqrt{\frac{2}{\gamma - 1}\left(\frac{p_2}{p_1}\right)^{1 - \frac{\gamma-1}{\eta\gamma}} \sqrt{1 + \frac{\gamma - 1}{2} M_{1_r}^2 - \left(\frac{p_2}{p_1}\right)^{\frac{\gamma-1}{\gamma\eta}}}} \tag{7}$$

By squaring and rearranging equations (6) and (7)

$$\left(\frac{p_2}{p_1}\right)^{\frac{\gamma-1}{\gamma\eta}} = 1 + \frac{\gamma - 1}{2} M_{1_r}{}^2 \left[1 - \left(\frac{V_{a_2}}{V_{a_1}}\right)^2 \frac{\cos^2\beta}{\cos^2(\beta - \theta)}\right] \tag{8}$$

By continuity

$$\frac{A_1}{A_2} = \frac{\rho_2}{\rho_1} \frac{V_{a_2}}{V_{a_1}} \tag{9}$$

Inasmuch as A_1/A_2 remains constant for off-design conditions and $\frac{\rho_2}{\rho_1} = f\left(\frac{p_2}{p_1},\eta\right)$, from equation (9) $\frac{V_{a_2}}{V_{a_1}} = f\left(\frac{p_2}{p_1},\eta\right)$; therefore, equation (8) has p_2/p_1 as an implicit function of M_{1_r}, η, β, and θ.

The inlet Mach number M_{1_r} may be expressed as a function of the velocity-diagram parameters which are shown in figure 4. In appendix B, M_{1_r} is derived as

$$M_{1_r} = \sqrt{\frac{V_{a_1}{}^2 + \left(U - V_{a_1} \tan\delta\right)^2}{\gamma R T_{1_s} - \frac{\gamma - 1}{2}\left(\frac{V_{a_1}}{\cos\delta}\right)^2}} \tag{10}$$

From figure 4

$$\cos^2\beta = \frac{V_{a_1}{}^2}{V_{a_1}{}^2 + \left(U - V_{a_1} \tan\delta\right)^2} \tag{11}$$

Combining equations (8), (10), and (11) gives $\frac{p_2}{p_1} = f\left(V_{a_1}, T_{l_s}, U, \delta, \theta, \eta\right)$:

$$\left(\frac{p_2}{p_1}\right)^{\frac{\gamma-1}{\gamma\eta}} = 1 + \frac{\gamma-1}{2} \frac{\left[V_{a_1}^2 + \left(U - V_{a_1} \tan \delta\right)^2\right] - V_{a_1}^2 \left(\frac{V_{a_2}}{V_{a_1}}\right)^2 \frac{1}{\cos^2(\beta - \theta)}}{\gamma R T_{l_s} - \frac{\gamma-1}{2}\left(\frac{V_{a_1}}{\cos \delta}\right)^2} \tag{12}$$

This equation defines the dashed curves in figure 3. It is an implicit equation in p_2/p_1 and η since V_{a_1}/V_{a_2} is also a function of p_2/p_1 and η. Equation (12) requires a trial-and-error solution.

The condition that $\frac{\rho_2}{\rho_1} = \left(\frac{\rho_2}{\rho_1}\right)_D$, that is, $\frac{V_{a_2}}{V_{a_1}} = \left(\frac{V_{a_2}}{V_{a_1}}\right)_D$, is specified by combining equations (4) and (12) and results in

$$\left(\frac{p_2}{p_1}\right)_D^{\left[\frac{1 - \frac{\gamma-1}{\gamma\eta_D}}{\frac{\gamma\eta_n}{\gamma-1} - 1}\right]} = 1 + \frac{\gamma-1}{2} \frac{\left[V_{a_1}^2 + \left(U - V_{a_1} \tan \delta\right)^2\right] - V_{a_1}^2 \left(\frac{V_{a_2}}{V_{a_1}}\right)_D^2 \frac{1}{\cos^2(\beta - \theta)}}{\gamma R T_{l_s} - \frac{\gamma-1}{2}\left(\frac{V_{a_1}}{\cos \delta}\right)^2} \tag{13}$$

This equation is the general expression for η_n as a function of the independent variables V_{a_1}, U, δ, θ, and T_{l_s}. The values of η_n can be found for the various off-design mass flows once the design conditions $\left(p_2/p_1\right)_D$, β_D, $\left(V_{a_2}/V_{a_1}\right)_D$, U_D, T_{l_s}, and η_D are selected. An algebraically simpler derivation for this equation is presented in

appendix C. The derivation employs static-temperature ratio alone, whereas the derivation developed in appendix B was made by utilizing the continuity equation, Mach numbers, and area ratios. The original derivation was presented because it led to several interesting relationships between Mach numbers, flow areas, and off-design pressure ratios.

Symmetrical Stage at Design Conditions and $\frac{d\theta}{d\beta} = 1$

The general equation presented in the previous section is applied to the case of a symmetrical stage. A symmetrical stage is defined herein as one in which $\beta - \theta = \delta$ and the axial velocity is constant. For a symmetrical stage, the over-all static-pressure ratio is approximately the square of the rotor static-pressure ratio. The following assumptions are made:

(1) The stage is symmetrical at design; that is, $\beta_D - \theta_D = \delta$ and $\left(\frac{V_{a_2}}{V_{a_1}}\right)_D = 1$

(2) $\frac{d\theta}{d\beta} = 1$; therefore, the off-design velocity diagrams will have $\beta - \theta = \delta$

(3) $T_{1_s} = \left(T_{1_s}\right)_D$

Equation (13) for the rotor static-pressure ratio becomes (see appendix B)

$$\left(\frac{p_2}{p_1}\right)_D^{\left[\frac{1-\frac{\gamma-1}{\gamma\eta_D}}{\frac{\gamma\eta_n}{\gamma-1}-1}\right]} = 1 + \frac{\frac{\gamma-1}{2}U\left(U - 2V_{a_1}\tan\delta\right)}{\gamma RT_{1_s} - \frac{\gamma-1}{2}\left(\frac{V_{a_1}}{\cos\delta}\right)^2} \tag{14}$$

Equation (14) presents $\eta_n = f\left[\eta_D, \left(\frac{p_2}{p_1}\right)_D, T_{1_s}, U, \delta, V_{a_1}\right]$ and will be investigated for various design pressure ratios.

The following table presents the design conditions for five rotors, all of which are symmetrical with constant axial velocity across the rotors at design:

$\left(\frac{p_2}{p_1}\right)_D$	$\beta_D - \theta_D = \delta$	$\left(V_{a_1}\right)_D$	M_1
1.30	13.8	612.0	0.88
1.25	18.6	575.0	.83
1.20	24.0	536.5	.77
1.15	30.0	497.0	.71
1.10	36.3	456.0	.65
1.05	43.1	413.3	.59

All designs have the following design parameters in common: $\beta_D = 50.0°$, $U_D = 879$ feet per second, and $\eta_D = 0.90$. Each design was investigated at $V_{a_1} = \left(V_{a_1}\right)_D$, $0.95\left(V_{a_1}\right)_D$, $0.90\left(V_{a_1}\right)_D$, $0.85\left(V_{a_1}\right)_D$, and $0.80\left(V_{a_1}\right)_D$, and the efficiency necessary to maintain the design density ratio, that is, axial-velocity ratio, was found for all the off-design conditions. Figure 5 is the plot of η_n against $V_{a_1}/\left(V_{a_1}\right)_D$ for the various design static-pressure ratios.

For a high-pressure-ratio stage, the reduction in η_n with decreasing axial-velocity ratio is more gradual than for a low-pressure-ratio stage. (See fig. 5.) The blade-row efficiency curves obtained from rotor tests (reference 4) tend to be in the region of the η_n curves for high pressure ratios (pressure ratios of the order of 1.4). Matching of η_n with the blade-row efficiency appears to be possible at the higher pressure ratios but almost impossible at low pressure ratios.

Since at high pressure ratios the η_n curves decrease less rapidly with decreasing axial velocity, the actual blade-row efficiency curve may be lower than the η_n curve associated with the design pressure ratio. Therefore, a multistage compressor with high over-all off-design efficiency (see fig. 2(b)) and a wide operating range would result.

Even if the blade-row efficiency is higher than the η_n curve associated with the design pressure ratio, the difference between them is less for the higher pressure-ratio designs. The reduction in axial velocity on proceeding through the compressor would, of course, be less

when the difference between $\eta_{\text{blade row}}$ and η_n was less. Therefore, the later stages of the compressor composed of high-pressure-ratio stages would be operating at higher axial velocities, hence, higher stage efficiencies, and at pressure ratios closer to design than its low-pressure-ratio counterpart. This compressor would have a higher over-all off-design efficiency.

Effect of Design Pressure Ratio on Off-Design Axial-Velocity Ratios with Constant Rotor Efficiency Assumed

In the analysis of the effect of design pressure ratio on off-design axial-velocity ratios, the following assumptions were made:

(1) The blade-row efficiency is constant at off-design axial velocities and equal to η_D

(2) The stage is symmetrical at design; that is, $\beta_D - \theta_D = \delta$ and $\left(\frac{V_{a_1}}{V_{a_2}}\right)_D = 1$

(3) $\frac{d\theta}{d\beta} = 1$; therefore, $\beta - \theta = \delta$ at off-design conditions

(4) $T_{1_s} = \left(T_{1_s}\right)_D$

With these assumptions, equation (12) becomes

$$\left(\frac{p_2}{p_1}\right)^{\frac{\gamma-1}{\gamma\eta_D}} = 1 + \frac{\gamma - 1}{2} \frac{U^2 - 2UV_{a_1} \tan \delta + V_{a_1}{}^2 \sec^2\delta \left[1 - \left(\frac{V_{a_2}}{V_{a_1}}\right)^2\right]}{\gamma RT_{1_s} - \frac{\gamma - 1}{2}\left(\frac{V_{a_1}}{\cos \delta}\right)^2} \tag{15}$$

Since

$$\left(\frac{p_2}{p_1}\right)^{1/n} = \frac{\rho_2}{\rho_1} \tag{16}$$

and

$$n = \frac{1}{1 - \frac{\gamma - 1}{\gamma \eta_D}} \tag{17}$$

substituting the value of n from equation (17) into equation (16) yields

$$\left(\frac{p_2}{p_1}\right)^{1 - \frac{\gamma-1}{\gamma \eta_D}} = \frac{\rho_2}{\rho_1} \tag{18}$$

By continuity

$$\frac{V_{a_2}}{V_{a_1}} = \frac{\rho_1 A_1}{\rho_2 A_2} \tag{19}$$

At design, $\left(\frac{V_{a_1}}{V_{a_2}}\right)_D = 1$; hence

$$\left(\frac{\rho_2}{\rho_1}\right)_D = \frac{A_1}{A_2} \tag{20}$$

Combining equations (16), (19), and (20) results in the following equation:

$$\frac{V_{a_2}}{V_{a_1}} = \left(\frac{\rho_2}{\rho_1}\right)_D \left(\frac{p_2}{p_1}\right)^{\frac{\gamma-1}{\gamma \eta_D} - 1} \tag{21}$$

By a trial-and-error solution, the off-design axial-velocity ratio V_{a_2}/V_{a_1} can be found for various off-design inlet axial velocities by using equations (15) and (21). Equation (15) can be solved for p_2/p_1 by choosing a value for V_{a_2}/V_{a_1}. When this value of p_2/p_1 is used

in equation (21), a new V_{a_2}/V_{a_1} can be found. The process is then repeated with this new value of V_{a_2}/V_{a_1} as the new initial value until the initial and calculated axial-velocity ratios are identical.

Figure 6 is a plot of $\frac{V_{a_1} - V_{a_2}}{(V_{a_1})_D}$ against $\frac{V_{a_1}}{(V_{a_1})_D}$ for various design pressure ratios with $\beta_D = 50.0^\circ$ and $U_D = 879$ feet per second. It shows that, when the off-design efficiency is assumed constant, the exit axial velocity goes farther from design for low design pressure ratios than for high design pressure ratios. For example, at 20 percent below design axial velocity when $\left(\frac{p_2}{p_1}\right)_D = 1.05$, $\frac{V_{a_1} - V_{a_2}}{(V_{a_1})_D} = 0.042$; whereas, for $\left(\frac{p_2}{p_1}\right)_D = 1.25$, $\frac{V_{a_1} - V_{a_2}}{(V_{a_1})_D} = 0.018$. The decrease in axial velocity across the low-pressure-ratio stage is over twice as great as that across the high-pressure-ratio stage. The 5.2-percent decrease in axial velocity calculated for the low-pressure-ratio stage is significant when it is realized that the reduction in axial velocity through a compressor is cumulative from stage to stage. Therefore, here again, for the same over-all design pressure ratio, the compressor with the high-pressure-ratio stages has a wider mass flow operating range since both the decrease in axial velocity per stage and the number of stages required are less in the compressor composed of high-pressure-ratio stages.

CONCLUSIONS

An analysis of the effects of design pressure ratio per stage and off-design stage efficiency on the operating range of multistage axial-flow compressors indicates the following conclusions:

1. The efficiency η_n necessary to maintain the design density ratio across a rotor, a stator, a stage, or several stages may be expressed as a function of the design efficiency and the design and off-design static-pressure ratios.

2. Inasmuch as the η_n curves for high-pressure-ratio stages (pressure ratios of the order of 1.4) lie in the region of typical efficiency curves obtained from test data, the stage efficiency and η_n can be

matched. If the stage efficiency matches η_n perfectly, the axial-velocity ratio across each blade row remains constant through the compressor for various off-design mass-flow conditions. If the stage efficiency is below η_n, the axial velocity increases somewhat through the compressor. In either case, the off-design over-all efficiency of the compressor is considerably higher and the operating range wider than that of a compressor made up of low-pressure-ratio stages.

3. Matching of η_n with the stage efficiency appears to be almost impossible for low-pressure-ratio stages. The curves of η_n presented in this paper for low-pressure-ratio stages are much steeper than curves of present-day blade-row-efficiency test data. Therefore, when a multistage compressor, composed of low-pressure-ratio stages with constant axial velocity at design, is operating at mass flows below design, the axial velocity decreases rapidly through the compressor. The operating range is limited by the later stages operating far from design axial velocity at low efficiencies.

4. Even if the η_n curves associated with a low-pressure-ratio stage and a high-pressure-ratio stage were both below the stage efficiency curve, assuming that the blade-row efficiency curves for the two pressure ratios were approximately the same, the multistage compressor composed of high-pressure-ratio stages would have higher over-all off-design efficiencies, a wider mass-flow operating range, and, in general, a flatter characteristic curve than one composed of low-pressure-ratio stages.

5. When the off-design stage efficiency is assumed constant, the axial velocity across a symmetrical rotor decreases more for low-pressure-ratio designs than for high-pressure-ratio designs. This result confirms the conclusion that the compressor with high-pressure-ratio stages has a wider operating range since the axial velocities are reduced less rapidly than in a compressor composed of low-pressure-ratio stages.

Langley Aeronautical Laboratory
National Advisory Committee for Aeronautics
Langley Field, Va., October 6, 1950

APPENDIX A

DETERMINATION OF EFFICIENCY NECESSARY TO MAINTAIN SAME DENSITY RATIO AS DESIGN AT OFF-DESIGN CONDITIONS

Let the ratio of off-design static-pressure ratio to design static-pressure ratio be denoted by

$$x = \frac{p_e/p_i}{(p_e/p_i)_D} \tag{A1}$$

For constant specific heat, the pressure ratio for the polytropic process is

$$\frac{p_e}{p_i} = \left(\frac{\rho_e}{\rho_i}\right)^n \tag{A2a}$$

$$\left(\frac{p_e}{p_i}\right)_D = \left(\frac{\rho_e}{\rho_i}\right)_D^{n_D} \tag{A2b}$$

Substituting equations (A2) into equation (A1) and, at the same time, making $\left(\frac{\rho_e}{\rho_i}\right)_D = \frac{\rho_e}{\rho_i}$ results in

$$x = \left(\frac{\rho_e}{\rho_i}\right)_D^{n-n_D} \tag{A3}$$

When equation (A2b) is substituted into equation (A3),

$$x = \left(\frac{p_e}{p_i}\right)_D^{\frac{n-n_D}{n_D}} \tag{A4}$$

By definition

$$n = \frac{1}{1 - \frac{1}{\eta}\frac{\gamma - 1}{\gamma}} \tag{A5a}$$

$$n_D = \frac{1}{1 - \frac{1}{\eta_D}\frac{\gamma - 1}{\gamma}} \tag{A5b}$$

Substituting equations (A5) into equation (A4) and denoting the efficiency necessary as η_n results in the following equation:

$$x = \left(\frac{p_e}{p_i}\right)_D^{\left[\frac{\frac{\gamma-1}{\gamma}\left(\frac{1}{\eta_n} - \frac{1}{\eta_D}\right)}{1 - \frac{1}{\eta_n}\frac{\gamma-1}{\gamma}}\right]} \tag{A6}$$

APPENDIX B

DETERMINATION OF EFFICIENCY NECESSARY TO MAINTAIN DESIGN DENSITY RATIO AT OFF-DESIGN CONDITIONS AS A FUNCTION OF OFF-DESIGN VELOCITY-DIAGRAM PARAMETERS

Preliminary Steps

Derivation of an expression for $\frac{p_2}{p_1} = f\left(M_{1_r}, \eta, \beta, \theta\right)$.- The temperature ratios at the rotor inlet and exit, respectively, are

$$\frac{T_{1_r}}{t_1} = 1 + \frac{\gamma - 1}{2} M_{1_r}^2 \tag{B1a}$$

$$\frac{T_{2_r}}{t_2} = 1 + \frac{\gamma - 1}{2} M_{2_r}^2 \tag{B1b}$$

If equations (B1) are expressed in terms of rotor coordinates, $T_{1_r} = T_{2_r}$; therefore,

$$\frac{t_2}{t_1} = \frac{1 + \frac{\gamma - 1}{2} M_{1_r}^2}{1 + \frac{\gamma - 1}{2} M_{2_r}^2} \tag{B2}$$

For constant specific heat, the temperature ratio for the polytropic process is

$$\frac{t_2}{t_1} = \left(\frac{p_2}{p_1}\right)^{\frac{n-1}{n}} = \left(\frac{p_2}{p_1}\right)^{\frac{1}{\eta}\frac{\gamma-1}{\gamma}} \tag{B3}$$

Substituting equation (B3) into equation (B2) yields the following equation:

$$\left(\frac{p_2}{p_1}\right)^{\frac{\gamma-1}{\eta\gamma}} = \frac{1 + \frac{\gamma - 1}{2} M_{1_r}^2}{1 + \frac{\gamma - 1}{2} M_{2_r}^2} \tag{B4}$$

The continuity equation can be written as follows:

$$\left(\frac{A_1}{A_2}\right)_f = \frac{\rho_2 W_2}{\rho_1 W_1} = \frac{\rho_2 V_{a_2} \cos \beta}{\rho_1 V_{a_1} \cos(\beta - \theta)} = \frac{\rho_2}{\rho_1} \frac{M_{2_r}}{M_{1_r}} \frac{\sqrt{t_2}}{\sqrt{t_1}} \tag{B5}$$

Substituting equations (B3), (A2a), and (A5a) into equation (B5) and solving for M_{2_r} results in

$$M_{2_r} = M_{1_r}\left(\frac{p_1}{p_2}\right)^{1 - \frac{\gamma-1}{2\eta\gamma}}\left(\frac{A_1}{A_2}\right)_f \tag{B6}$$

Substituting equation (B6) into equation (B4) and solving for $\left(\frac{A_1}{A_2}\right)_f$ yields

$$\left(\frac{A_1}{A_2}\right)_f = \frac{1}{M_{1_r}}\sqrt{\frac{2}{\gamma - 1}}\left(\frac{p_2}{p_1}\right)^{1 - \frac{\gamma-1}{\eta\gamma}} \sqrt{1 + \frac{\gamma - 1}{2} M_{1_r}^2 - \left(\frac{p_2}{p_1}\right)^{\frac{\gamma-1}{\eta\gamma}}} \tag{B7}$$

Substituting equation (B7) into equation (B5) and then squaring results in

$$\frac{\cos^2\beta}{\cos^2(\beta - \theta)} = \frac{2}{\gamma - 1}\left(\frac{\rho_1}{\rho_2}\right)^2\left[\left(\frac{p_2}{p_1}\right)^2\right]^{1 - \frac{\gamma-1}{\eta\gamma}}\left(\frac{V_{a_1}}{V_{a_2}}\right)^2 \frac{1}{M_{1_r}^2}\left[1 + \frac{\gamma - 1}{2} M_{1_r}^2 - \left(\frac{p_2}{p_1}\right)^{\frac{\gamma-1}{\eta\gamma}}\right] \tag{B8}$$

Substituting equations (A2a) and (A5a) into equation (B8) and rearranging yields

$$\left(\frac{p_2}{p_1}\right)^{\frac{\gamma-1}{\eta\gamma}} = 1 + \frac{\gamma - 1}{2} M_{1_r}{}^2 \left[1 - \left(\frac{V_{a_2}}{V_{a_1}}\right)^2 \frac{\cos^2\beta}{\cos^2(\beta - \theta)}\right] \tag{B9}$$

Since $\frac{V_{a_2}}{V_{a_1}} = f\left(\frac{\rho_2}{\rho_1}, \frac{A_1}{A_2}\right)$ by continuity and since $\frac{\rho_2}{\rho_1} = f\left(\frac{p_2}{p_1}, \eta\right)$ and A_1/A_2 is constant at off-design conditions, equation (B9) is the expression for $\frac{p_2}{p_1} = f\left(M_{1_r}, \eta, \beta, \theta\right)$.

Derivation of an expression for $M_{1_r} = f\left(V_{a_1}, U, \delta, T_{1_s}\right)$.- In order to express M_{1_r} as a function of the velocity-diagram parameters, it can be seen from figure 4 that

$$W_1{}^2 = V_{a_1}{}^2 + \left(U - V_{a_1} \tan \delta\right)^2 \tag{B10}$$

The temperature ratio in stator coordinates is

$$\frac{T_{1_s}}{t_1} = 1 + \frac{\gamma - 1}{2} M_{1_s}{}^2 \tag{B11}$$

Substituting $\left(\frac{V_{a_1}}{\cos \delta}\right)\frac{1}{a_1}$ for M_{1_s} in equation (B11) and solving for a_1 gives

$$a_1 = \sqrt{\gamma R T_{1_s} - \frac{\gamma - 1}{2}\left(\frac{V_{a_1}}{\cos \delta}\right)^2} \tag{B12}$$

Dividing equation (B10) by a_1^2 gives

$$M_{1_r}^2 = \frac{V_{a_1}^2 + \left(U - V_{a_1} \tan \delta\right)^2}{\gamma R T_{1_s} - \frac{\gamma - 1}{2}\left(\frac{V_{a_1}}{\cos \delta}\right)^2} \tag{B13}$$

Application of the Condition that η be Equal to η_n

In the application of the condition that η be equal to η_n, the procedure is as follows: From figure 4

$$\cos^2\beta = \frac{V_{a_1}^2}{V_{a_1}^2 + \left(U - V_{a_1} \tan \delta\right)^2} \tag{B14}$$

Combining equations (B9), (B13), and (B14) results in

$$\left(\frac{p_2}{p_1}\right)^{\frac{\gamma-1}{\gamma\eta}} = 1 + \frac{\gamma - 1}{2} \frac{\left[V_{a_1}^2 + \left(U - V_{a_1} \tan \delta\right)^2\right] - \frac{V_{a_2}^2}{\cos^2(\beta - \theta)}}{\gamma R T_{1_s} - \frac{\gamma - 1}{2}\left(\frac{V_{a_1}}{\cos \delta}\right)^2} \tag{B15}$$

From equations (A6) and (A1)

$$\frac{p_2}{p_1} = \left(\frac{p_2}{p_1}\right)_D^{\left[\frac{1 - \frac{\gamma-1}{\gamma\eta_D}}{1 - \frac{\gamma-1}{\gamma\eta_n}}\right]} \tag{B16}$$

Substituting equation (B16) into equation (B15) and at the same time realizing that $\frac{V_{a_2}}{V_{a_1}} = \left(\frac{V_{a_2}}{V_{a_1}}\right)_D$ results in the following equation:

$$\left(\frac{p_2}{p_1}\right)_D^{\left[\frac{1-\frac{\gamma-1}{\gamma\eta_D}}{\frac{\gamma\eta_n}{\gamma-1}-1}\right]} = 1 + \frac{\gamma-1}{2}\frac{\left[V_{a_1}^2 + \left(U - V_{a_1}\tan\delta\right)^2\right] - V_{a_1}^2\left(\frac{V_{a_2}}{V_{a_1}}\right)_D^2 \frac{1}{\cos^2(\beta-\theta)}}{\gamma R T_{1_s} - \frac{\gamma-1}{2}\left(\frac{V_{a_1}}{\cos\delta}\right)^2} \tag{B17}$$

This equation is the general expression for

$$\eta_n = f\left(V_{a_1}, U, \delta, \theta, T_{1_s}\right)$$

Special Case of Equation (B17) for $\left(\frac{V_{a_2}}{V_{a_1}}\right)_D = 1$, $\frac{d\theta}{d\beta} = 1$, and Symmetrical Stage at Design

For a symmetrical stage, assuming $\frac{d\theta}{d\beta} = 1$ means that the off-design velocity diagrams will also have

$$\beta - \theta = \delta \tag{B18}$$

Combining equations (B17) and (B18), assuming $\left(V_{a_1}\right)_D = \left(V_{a_2}\right)_D$, and simplifying yields

$$\left(\frac{p_2}{p_1}\right)_D^{\left[\frac{1-\frac{\gamma-1}{\gamma\eta_D}}{\frac{\gamma\eta_n}{\gamma-1}-1}\right]} = 1 + \frac{\frac{\gamma-1}{2}U\left(U - 2V_{a_1}\tan\delta\right)}{\gamma R T_{1_s} - \frac{\gamma-1}{2}\left(\frac{V_{a_1}}{\cos\delta}\right)^2} \tag{B19}$$

APPENDIX C

ALTERNATE DERIVATION OF EQUATION (B17)

At design conditions

$$\left(\frac{p_2}{p_1}\right)_D = \left(\frac{\rho_2}{\rho_1}\right)_D^{n_D} \tag{C1}$$

At off-design conditions

$$\frac{p_2}{p_1} = \left(\frac{\rho_2}{\rho_1}\right)^n \tag{C2}$$

To keep $\frac{V_{a_1}}{V_{a_2}} = \left(\frac{V_{a_1}}{V_{a_2}}\right)_D$

$$\frac{\rho_2}{\rho_1} = \left(\frac{\rho_2}{\rho_1}\right)_D \tag{C3}$$

Therefore,

$$\frac{p_2}{p_1} = \left(\frac{p_2}{p_1}\right)_D^{n/n_D} \tag{C4}$$

But

$$\frac{p_2}{p_1} = \left(\frac{t_2}{t_1}\right)^{\frac{n}{n-1}} \tag{C5}$$

where

$$n = \frac{\eta}{\eta - \frac{\gamma - 1}{\gamma}} \tag{C6}$$

Combining equations (C4), (C5), and (C6) yields

$$\frac{t_2}{t_1} = \left(\frac{p_2}{p_1}\right)_D^{\left[\frac{1-\frac{\gamma-1}{\eta_D\gamma}}{\frac{\gamma\eta}{\gamma-1}-1}\right]} \tag{C7}$$

Since

$$t_2 = T_{2_r} - \frac{W_2^2}{2c_p} \tag{C8}$$

$$T_{2_r} = T_{1_r} = t_1 + \frac{W_1^2}{2c_p} \tag{C9}$$

and from figure 4

$$W_2^2 = \frac{V_{a_2}^2}{\cos^2(\beta - \theta)} \tag{C10}$$

$$W_1^2 = V_{a_1}^2 + \left(U - V_{a_1} \tan \delta\right)^2 \tag{C11}$$

Combining equations (C8) to (C11) gives

$$\frac{t_2}{t_1} = 1 + \frac{V_{a_1}^2 + \left(U - V_{a_1} \tan \delta\right)^2 - \frac{V_{a_2}^2}{\cos^2(\beta - \theta)}}{2c_p t_1} \tag{C12}$$

Equating (C7) and (C12) results in the following equation:

$$\left(\frac{p_2}{p_1}\right)_D^{\left[\frac{1-\frac{\gamma-1}{\eta_D\gamma}}{\frac{\gamma\eta}{\gamma-1}-1}\right]} = 1 + \frac{V_{a_1}^2 + \left(U - V_{a_1}\tan\delta\right)^2 - \frac{V_{a_2}^2}{\cos^2(\beta-\theta)}}{2c_p t_1} \quad (C13)$$

This equation is equivalent to equation (B17) since $t_1 = T_{1_s} - \frac{1}{2c_p}\left(\frac{V_{a_1}}{\cos\delta}\right)^2$, $V_{a_2}^2 = V_{a_1}^2\left(\frac{V_{a_2}}{V_{a_1}}\right)_D^2$, and the η used is actually η_n.

REFERENCES

1. Bogdonoff, Seymour M.: The Performance of Axial-Flow Compressors as Affected by Single Stage Characteristics. Rep. No. 155, Princeton Univ., Aero. Eng. Lab., Oct. 1, 1949.

2. Sinnette, John T., Jr.: Analysis of Effect of Basic Design Variables on Subsonic Axial-Flow-Compressor Performance. NACA Rep. 901, 1948.

3. Bogdonoff, Seymour M., and Herrig, L. Joseph: Performance of Axial-Flow Fan and Compressor Blades Designed for High Loadings. NACA TN 1201, 1947.

4. Herrig, L. Joseph, and Bogdonoff, Seymour M.: Performance of an Axial-Flow Compressor Rotor Designed for a Pitch-Section Lift Coefficient of 1.20. NACA TN 1388, 1947.

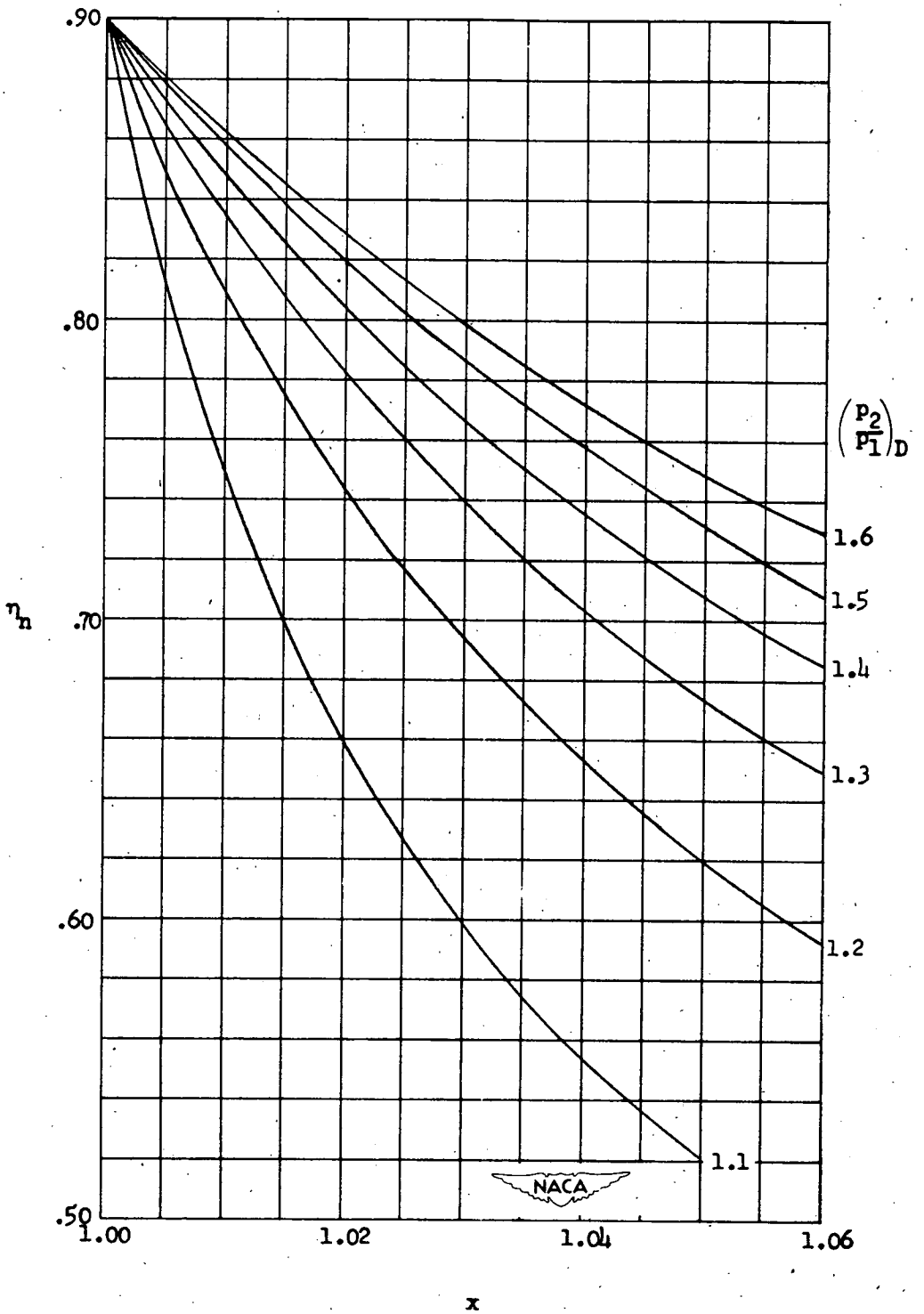

Figure 1.- Efficiency necessary to maintain design axial-velocity ratio at various off-design inlet axial velocities as a function of ratio of off-design static-pressure ratio to design static-pressure ratio for various design static-pressure ratios. $\eta_D = 0.90$.

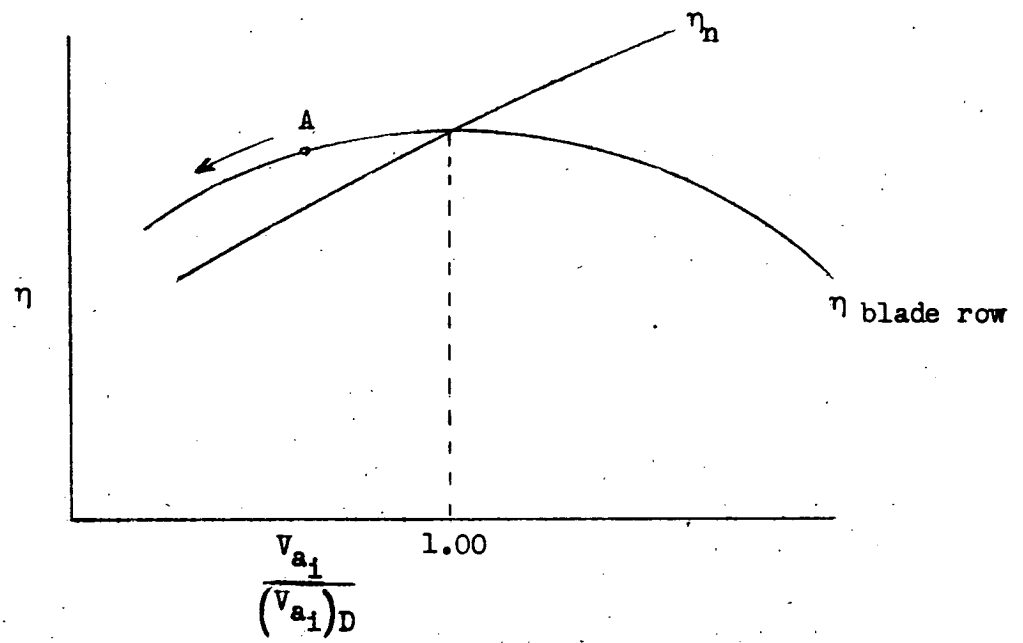

(a) η_n < Blade-row efficiency for $\frac{V_{a_i}}{(V_{a_i})_D} < 1.00$.

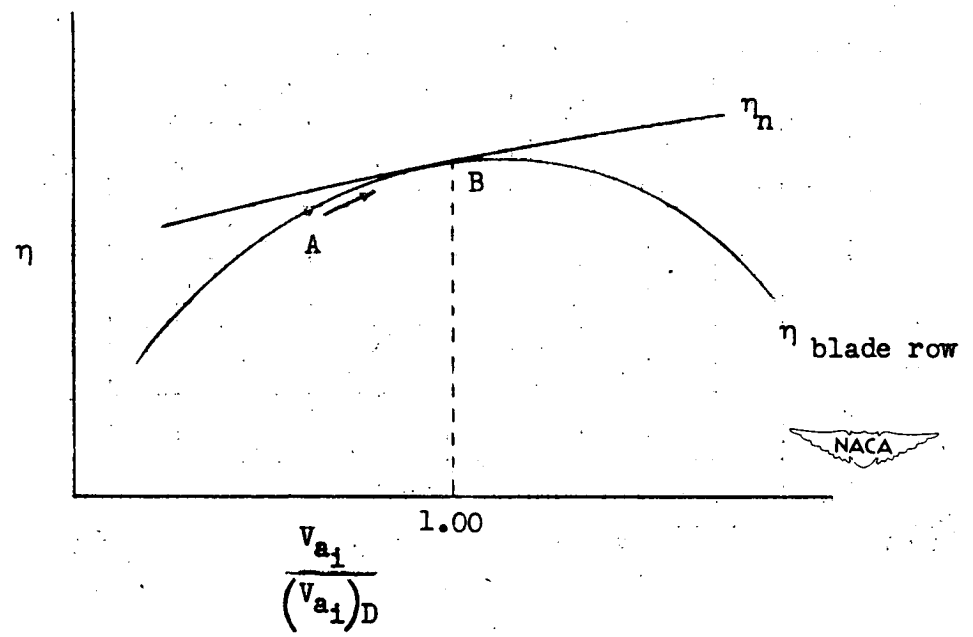

(b) η_n > Blade-row efficiency.

Figure 2.- The effects of the relative magnitudes of η_n and $\eta_{\text{blade row}}$ on the exit axial velocity of a rotor.

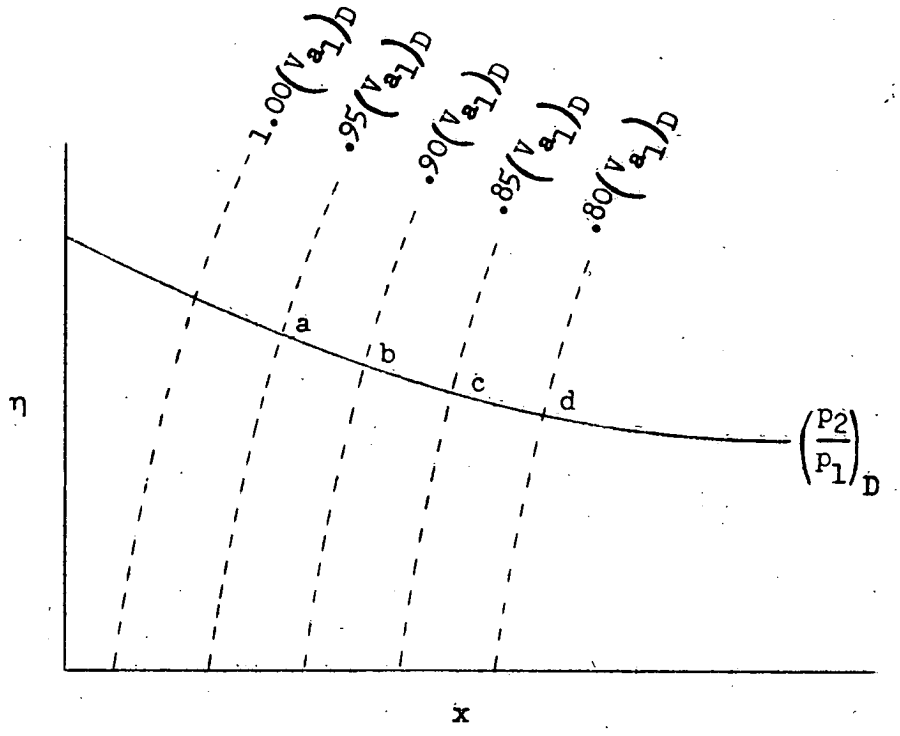

Figure 3.- Variation of η_n with x for a specific design static-pressure ratio, solid curve. Functional relationship between x, efficiency, and off-design inlet axial velocity, dashed curves.

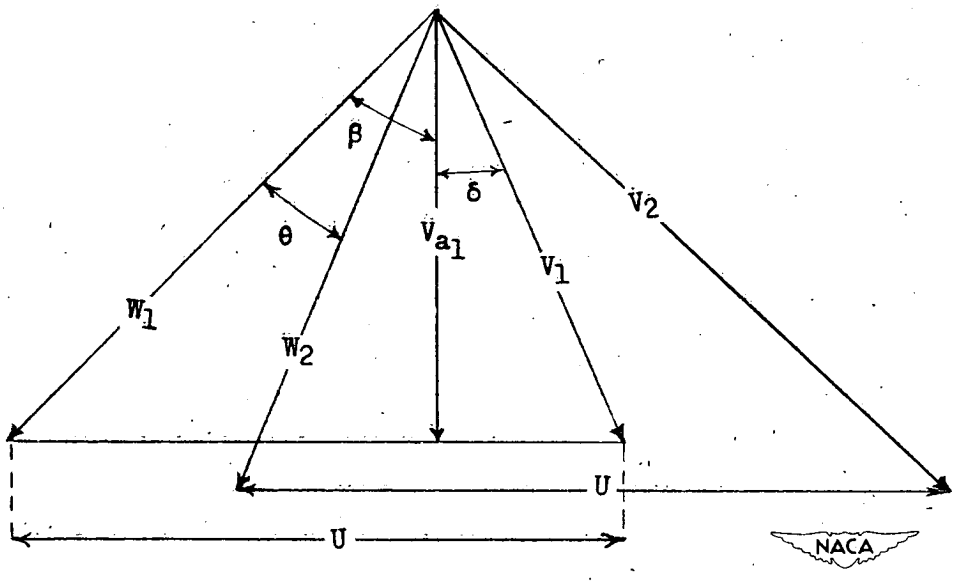

Figure 4.- Velocity diagram of stage.

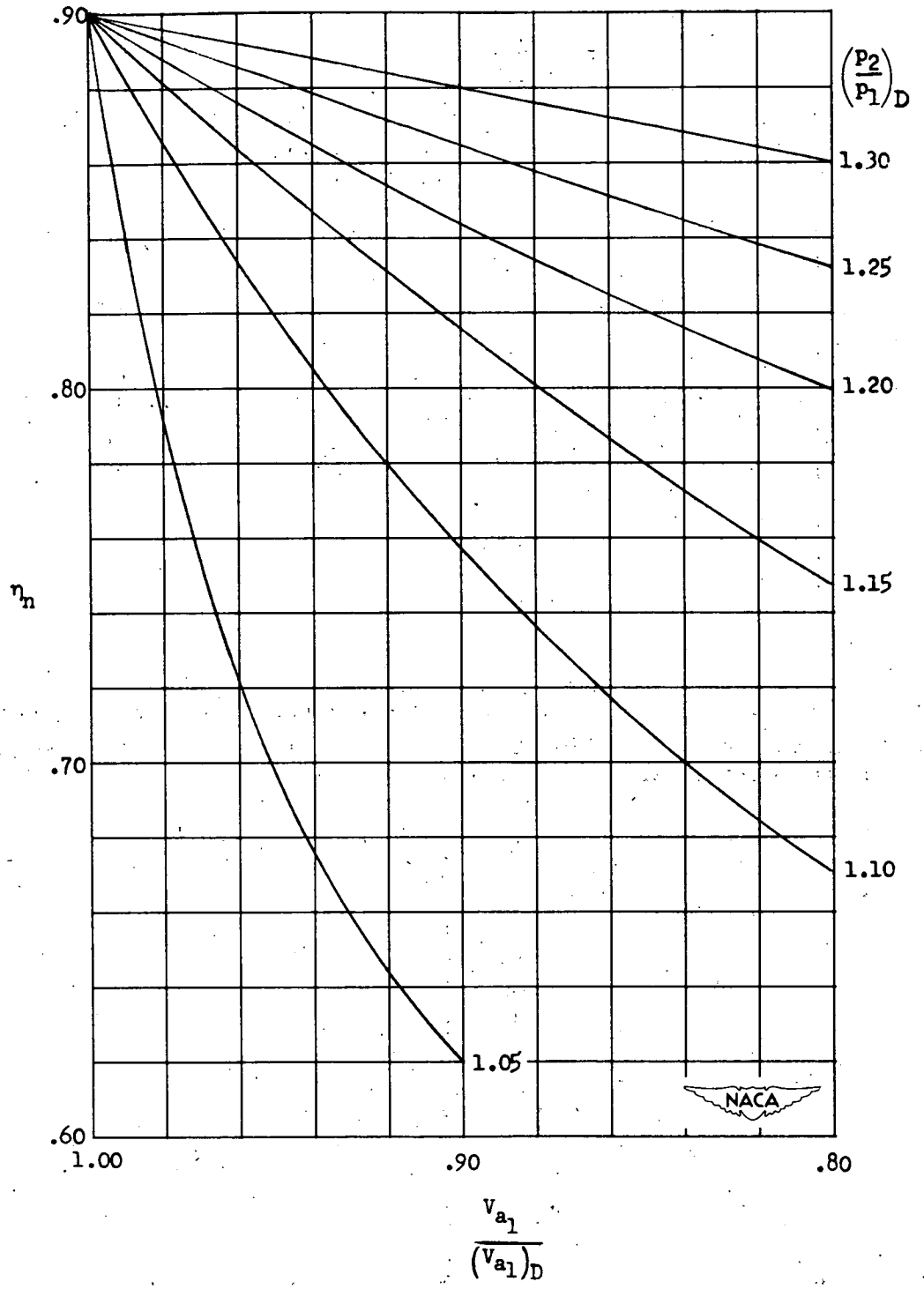

Figure 5.- Efficiency η_n as a function of $\frac{V_{a_1}}{(V_{a_1})_D}$ for several values of design pressure ratio. $\beta_D = 50.0^\circ$ and $U_D = 879$ feet per second.

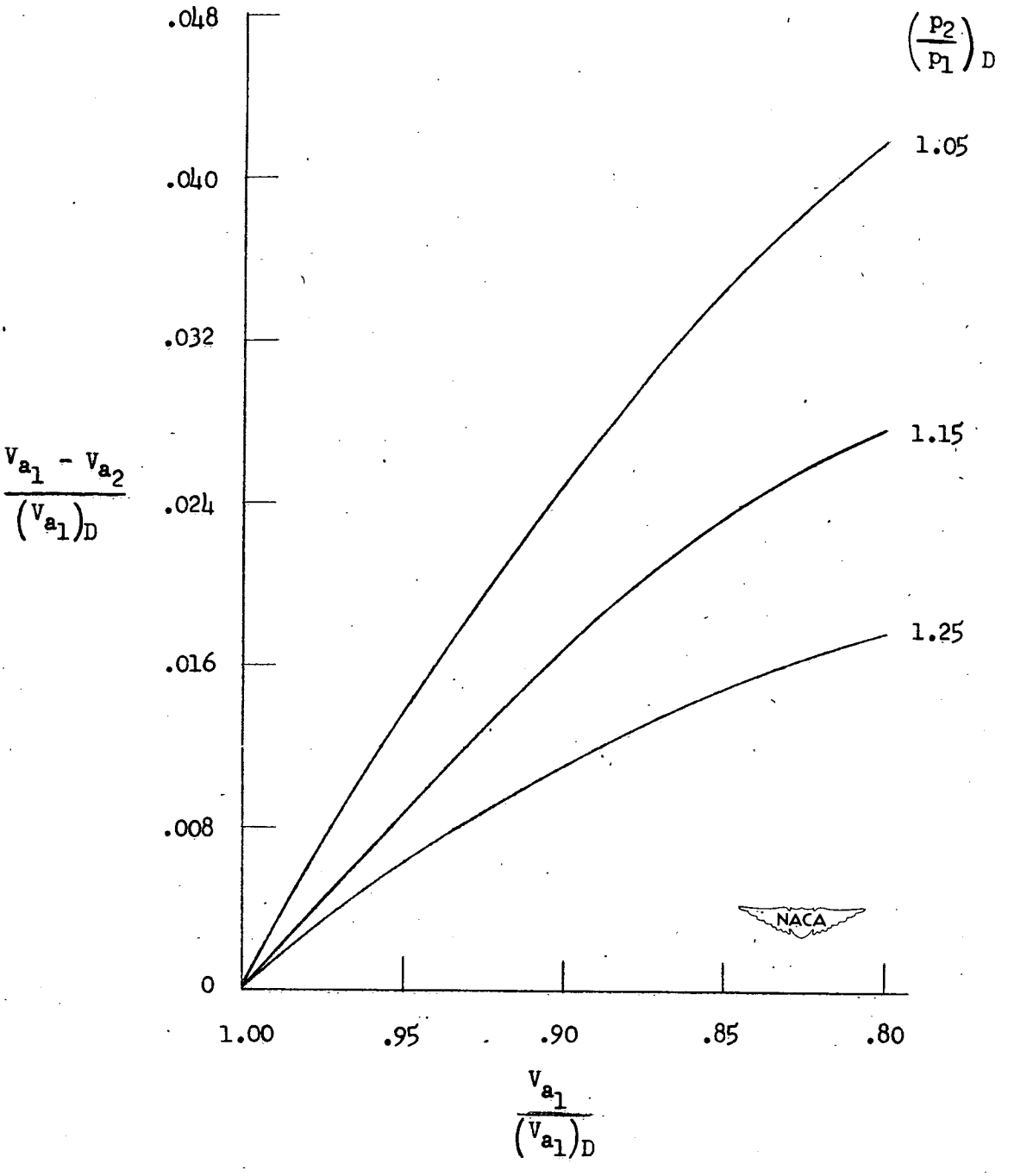

Figure 6.- Ratio of the change in axial velocity across a symmetrical rotor to the design inlef axial velocity as a function of $\frac{V_{a_1}}{(V_{a_1})_D}$ for several design pressure ratios. Blade-row efficiency assumed constant and equal to 0.90. $\beta_D = 50.0^\circ$ and $U_D = 879$ feet per second.